Semiannual Technical Report

Nitride Semiconductors for Ultraviolet Detection

Supported under Grant #N00014-92-J-1720
Office of the Chief of Naval Research
Report for the period January 1, 1994–June 30, 1994

R. F. Davis, K. Linthicum, B. Perry, C. Wang and W. Weeks
Materials Science and Engineering Department
North Carolina State University
Campus Box 7907
Raleigh, NC 27695-7907

June, 1994

REPORT DOCUMENTATION PAGE

Form Approved
OMB No. 0704-0188

1. AGENCY USE ONLY *(Leave blank)*	2. REPORT DATE	3. REPORT TYPE AND DATES COVERED
	June, 1994	Semiannual Technical 1/1/94–6/30/94

4. TITLE AND SUBTITLE

Nitride Semiconductors for Ultraviolet Detection

5. FUNDING NUMBERS

s400018srr01
1114SS
N00179
N66005
4B855

6. AUTHOR(S)

Robert F. Davis

7. PERFORMING ORGANIZATION NAME(S) AND ADDRESS(ES)

North Carolina State University
Hillsborough Street
Raleigh, NC 27695

8. PERFORMING ORGANIZATION REPORT NUMBER

N00014-92-J-1720

9. SPONSORING/MONITORING AGENCY NAMES(S) AND ADDRESS(ES)

Sponsoring: ONR, Code 314, 800 N. Quincy, Arlington, VA 22217-5660
Monitoring: Office of Naval Research Resider
The Ohio State University Research Center
1960 Kenny Road
Columbus, OH 43210-1063

10. SPONSORING/MONITORING AGENCY REPORT NUMBER

11. SUPPLEMENTARY NOTES

12a. DISTRIBUTION/AVAILABILITY STATEMENT

Approved for Public Release; Distribution Unlimited

12b. DISTRIBUTION CODE

13. ABSTRACT *(Maximum 200 words)*

Monocrystalline GaN thin films have been grown on vicinal α(6H)-SiC(0001) and sapphire(0001) wafers via organometallic vapor phase epitaxy (OMVPE) using a cold-wall, vertical barrel reactor with triethylgallium (TEG) and ammonia. Chemical, analytical and microstructural studies revealed epitaxial films of high microstructural quality. The surface morphologies and photoluminescence spectroscopy (PL) spectra of GaN films on both substrates are presented and described. Specifically, the PL data revealed donor bound exciton emission at 357.6 nm for films thicker than 1 mm. Two other emission peaks at 375-378 nm and 540 nm were common to all films tested. Hall effect measurements showed that the unintentionally doped films were highly n-type with a mobility of ≈40 $cm^2/V \cdot s$. The new method for the growth of the III-V compounds, namely, the use on an ammonia cracker cell to minimize film damage and increase growth rate has been designed and ordered. Preliminary studies of the use of AlN as a candidate insulator material has been conducted via the fabrication of an MIS structure. I-V and high frequency C-V measurements revealed a 13.4 MV/cm breakdown field and a dielectric constant of ~14. Operation of the MIS devices at 300°C with only a slight reduction in the breakdown field to 13 MV/cm.

14. SUBJECT TERMS

GaN, α(6H)-SiC(0001), OMVPE, vapor phase epitaxy, photoluminescence spectroscopy, donor bound emission, Hall effect, MIS device, breakdown field, dielectric constant

15. NUMBER OF PAGES

23

16. PRICE CODE

17. SECURITY CLASSIFICATION OF REPORT	18. SECURITY CLASSIFICATION OF THIS PAGE	19. SECURITY CLASSIFICATION OF ABSTRACT	20. LIMITATION OF ABSTRACT
UNCLAS	UNCLAS	UNCLAS	SAR

Table of Contents

I. Introduction

Continued development and commercialization of optoelectronic devices, including light-emitting diodes and semiconductor lasers produced from III–V gallium arsenide-based materials, has also generated interest in the much wider bandgap semiconductor mononitride materials containing aluminum, gallium, and indium. The majority of the studies have been conducted on pure gallium nitride thin films having the wurtzite structure, and this emphasis continues to the present day. Recent research has resulted in the fabrication of p–n junctions in wurtzitic gallium nitride, the deposition of cubic gallium nitride, as well as the fabrication of multilayer heterostructures and the formation of thin film solid solutions. Chemical vapor deposition (CVD) has usually been the technique of choice for thin film fabrication. However, more recently these materials have also been deposited by plasma-assisted CVD and reactive and ionized molecular beam epitaxy.

The program objectives in this reporting period have been (1) the growth of monocrystalline GaN thin films on vicinal α(6H)-SiC(0001) and sapphire(0001) wafers via organometallic vapor phase epitaxy (OMVPE), (2) chemical, analytical, microstructural, electrical and photoluminescence spectroscopic characterization of these films, and (3) the design of an ammonia cracker cell for high flux growth. Preliminary studies of the use of AlN as a candidate insulator material has been conducted via the fabrication of an MIS structure. I-V and high frequency C-V measurements revealed a 13.4 MV/cm breakdown field and a dielectric constant of ~14. Operation of the MIS devices at 300°C with only a slight reduction in the breakdown field to 13 MV/cm.

The procedures, results, discussions of these results and conclusions of these studies are summarized in the following sections with reference to appropriate SDIO/ONR reports for details. Note that each major section is self-contained with its own figures, tables and references.

II. Growth and Characterization of GaN Thin Films Grown by OMVPE

A. Introduction

The potential semiconductor and optoelectronic applications of the wide bandgap III-V nitrides has prompted significant research into their growth and development. GaN (wurtzite structure), the most studied in this group, has a bandgap of 3.4 eV and forms continuous solid solutions with both AlN (6.2 eV) and InN (1.9 eV). As such, materials with engineered bandgaps are envisioned for optoelectronic devices tunable from the visible to deep UV frequencies. An AlGaN/InGaN/AlGaN double heterostructure-base blue LED is now commercially available in Japan. The relatively strong atomic bonding of these materials also points to their potential use in high-power and high-temperature devices.

Single crystal wafers of GaN do not exist [1]. Sapphire(0001) is the most commonly used substrate, although its lattice parameter and coefficient of thermal expansion are different than that of GaN. The use of low temperature (450°C-600°C) buffer layers of AlN [2-5] or GaN [6,7] has resulted in improved GaN film quality and surface morphology. Undoped GaN is n-type. To date, p-type behavior has been achieved in chemically vapor deposited Mg- or Zn-doped GaN using either low-energy electron beam irradiation [8] or via thermal annealing in a N_2 atmosphere [9]. Acceptor-type behavior has been obtained directly in molecular beam epitaxially grown films [10].

In the present research, monocrystalline GaN films have been grown directly on vicinal, n-type α(6H)-SiC(0001)$_{Si}$ wafers via organometallic vapor phase epitaxy (OMVPE) in a cold-wall, vertical barrel reactor. GaN film growth on vicinal SiC(0001)$_C$ wafers and sapphire(0001) was also investigated. Triethylgallium (TEG) and ammonia where used as the reactants. The heteroepitaxial growth of GaN on SiC was characterized using reflection high-energy electron diffraction (RHEED), scanning electron microscopy (SEM), transmission electron microscopy (TEM), photoluminescence spectroscopy (PL) and X-ray rocking curve (XRC) and Hall-effect measurements. The following sections describe the experimental procedures, detail the results, provide a discussion and conclusions regarding this research and outline future research plans and goals.

B. Experimental Procedure

GaN thin films were grown directly on off-axis SiC(0001) and sapphire(0001) substrates at 900°C. Low-temperature buffers layers were not employed in this study. The as-received vicinal SiC and sapphire wafers were cut into 7.1 mm squares. The SiC pieces were degreased, dipped into a 10% HF solution for 10 minutes to remove the thermally grown oxide layer and blown dry with N_2 before being loaded onto the barrel-style, SiC-coated graphite susceptor. For the sapphire substrates, prior to being HF dipped, they were cleaned

for 10 minutes in a hot H_2SO_4:H_3PO_4 solution. The reactor was evacuated to $<3\times10^{-5}$ torr for one hour prior to initiating growth. The continuously rotating susceptor was heated to 900°C by rf induction in 1.5 slm of flowing N_2. Nitrogen was also used as the diluent and as the TEG carrier gas. The flow rates of TEG, NH_3 and N_2 diluent were 14.75 μmol/min, 500 sccm and 1.5 slm, respectively. The system pressure during growth was 45 torr.

The structural, microstructural, optical and electrical characteristics of the epitaxial GaN thin films were analyzed using several techniques. SEM was performed on a JEOL 6400FE operating at 2 kV. The XRCs were obtained using a double-crystal X-ray diffractometer (Siemens D5000) with $CuK_{\alpha 1}$ line (1.54094Å) as the X-ray source. XRCs were recorded by plotting the diffracted intensity measured with a scintillation counter versus the specimen crystal rotation angle ω [11]. Conventional and high resolution TEM was performed on a JEOL 4000EX microscope operating at 400 kV. The photoemission properties of the unintentionally doped GaN films of varying thicknesses on vicinal SiC(0001) substrates were determined using low-temperature (T = 20K) PL obtained using a 15 mW He-Cd laser (325 nm) as the excitation source. GaN films grown on sapphire(0001) with no buffer layer were analyzed for comparative purposes. The unintentionally doped GaN films were characterized by Hall-effect measurements using the Van der Pauw geometry. Thermally evaporated Al was used as the contacts to these films with only linear regions of the current-voltage (I-V) curves being used for taking the Hall measurements.

C. Results and Discussion

A TEM micrograph of an 0.36 μm unintentionally doped GaN film on $SiC(0001)_{Si}$ is shown in Fig. 1. RHEED patterns for GaN grown on the $SiC(0001)_{Si}$ are displayed in Fig. 2.

Figure 1. TEM micrograph of GaN grown directly on $SiC(0001)_{Si}$ at 900°C by OMVPE.

(a) (b)

Figure 2. RHEED patterns for GaN grown on $SiC(0001)_{Si}$ at 900°C showing the (a) $[11\bar{2}0]$ and (b) $[10\bar{1}0]$ azimuths.

The former shows that the defect density diminishes as film thickness increases. The apparent vertical threading dislocations are believed to originate at the steps in the vicinal SiC surface as a result of the incompatibilities between the ABCACB... stacking sequence of (6H)-SiC and the ABABAB... sequence of (2H)-GaN. Any misalignment at these dislocations is very small, as the lattice images of the GaN bilayers traverse these threading dislocations without loss of contrast.

For the GaN films, XRC data revealed full width at half maximum (FWHM) values as low as 144 arcsec for the GaN(0002) reflection (Fig. 3). The sample from which Fig. 1 was obtained had a value of 148 arcsec for this reflection. In conjunction with the TEM images, these low FWHM values indicate that the film quality of GaN directly on SiC without a buffer layer is at least equal to that of GaN/buffer layer/sapphire(0001) films [12].

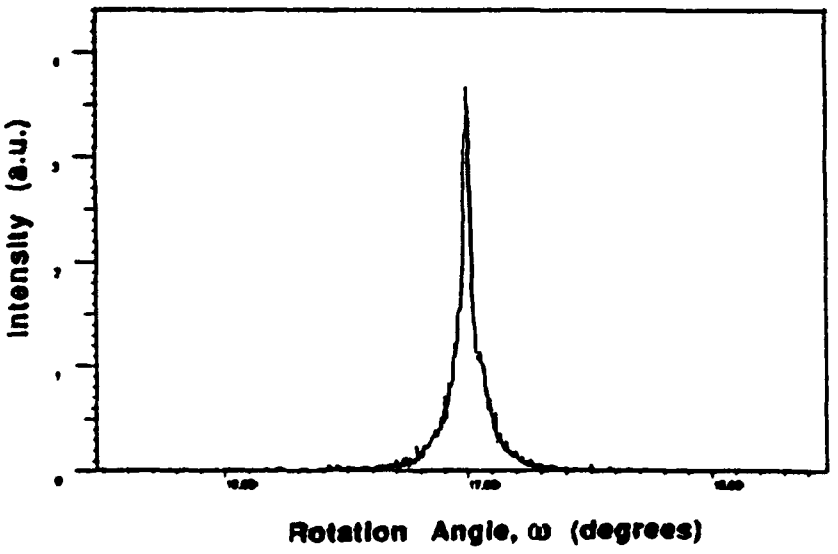

Figure 3. X-ray rocking curve for the GaN(0002) reflection. The FWHM value is 144 arcsec.

The low-temperature PL spectra of the various films are shown in Fig. 4. The lowest wavelength (highest energy) peaks are near-band-edge emissions. These quasi-I_2 lines centered around 357 nm for the thicker films [Fig. 4(D) and (F)] are attributed to the recombinations of excitons bound to neutral donors. The second group of peaks located at higher wavelengths are tentatively assigned to donor-acceptor (DA) transitions [13]. Figure 4 shows the PL peaks of GaN on $SiC(0001)_{Si}$ tend to shift to higher wavelengths (lower energies) with decreasing GaN film thickness. The peak intensities have been scaled appropriately to better facilitate graphical representation. The observed peak shifts are attributed to residual strain in the GaN lattice on SiC at reduced film thicknesses [14]. As the GaN films become thicker, the quality of the volume of material analyzed by PL improves. Thus, the shift in the PL signals originating from the highly defected interfacial region of the GaN/SiC films are not observed in the thicker films. With the large lattice mismatch between GaN and sapphire, strain is relaxed immediately and does not distort the PL spectra as strongly. The residual stress in the GaN/SiC becomes relieved as film thickness increases. Only the thicker 1.2 μm GaN/SiC film [Fig. 4(D)] has PL peaks similar to the GaN/sapphire films [Figs. 4(E) and (F)].

GaN films grown on the different polar planes of SiC(0001), namely the Si- and C-faces, had dissimilar surface morphologies as can be seen in Figs. 5 and 6, respectively. Using X-ray photoelectron spectroscopy, Sasaki [15] determined that GaN polarity changes in

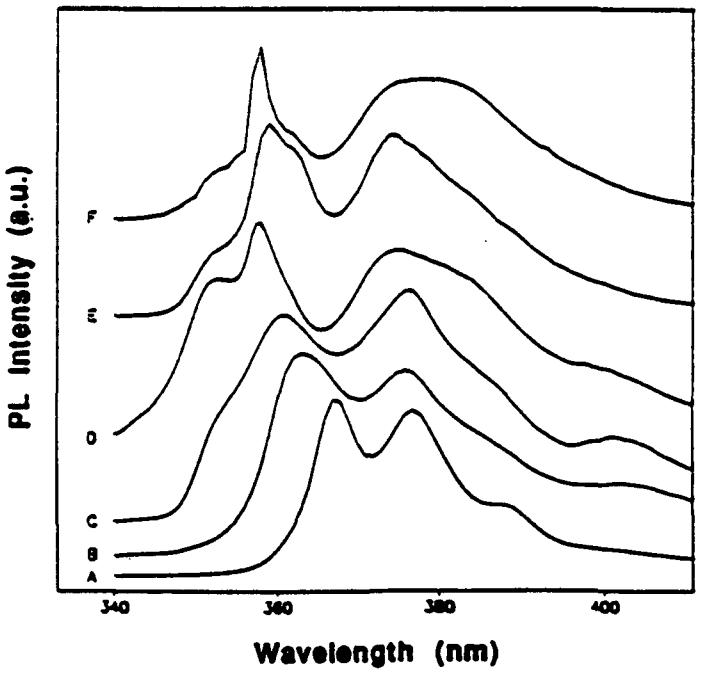

Figure 4. Low-temperature (T = 20K) PL spectra comparing (A) 0.21 μm (B) 0.36 μm (C) 0.5 μm and (D) 1.2 μm GaN films on $SiC(0001)_{Si}$ with (E) 0.24 μm and (F) 1.2 μm GaN films on sapphire.

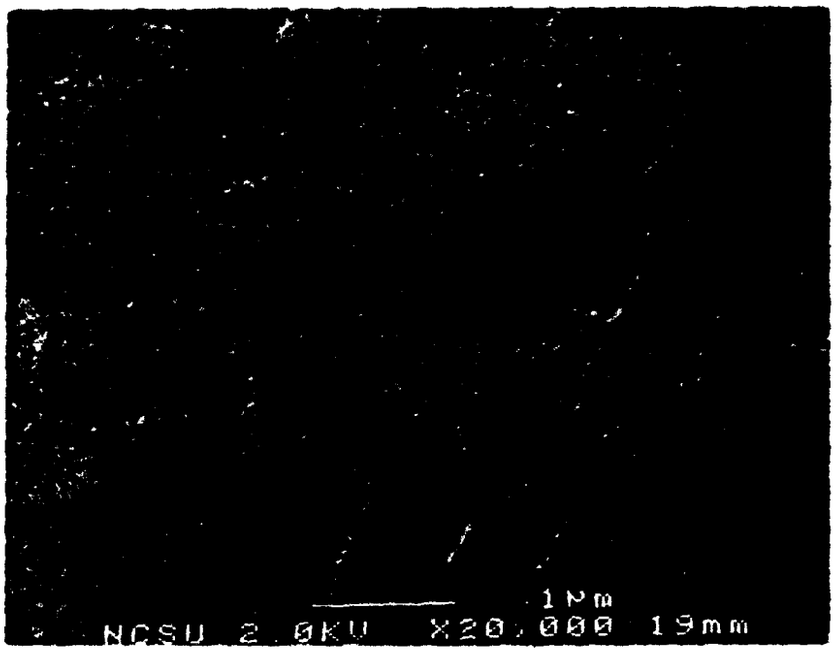

Figure 5. SEM micrograph of GaN deposited on $SiC(0001)_{Si}$ at 900°C.

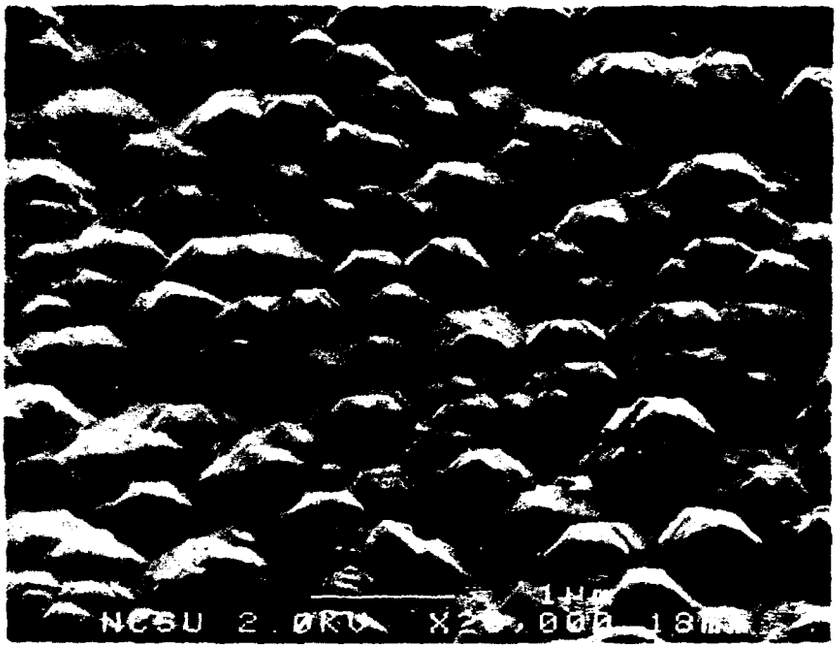

Figure 6. SEM micrograph of GaN deposited on $SiC(0001)_C$ at 900°C.

accordance with the substrate polarity. He estimated that GaN films grown on sapphire and $SiC(0001)_C$ were Ga terminated whereas films deposited on $SiC(0001)_{Si}$ were N terminated. In agreement with Sasaki's findings, the present research revealed the surface morphologies

and PL spectra of GaN films on sapphire and the C-face wafers were similar to each other but unlike those of films deposited on the Si-face substrates. Although not shown, the PL spectrum for GaN deposited on $SiC(0001)_C$ is nearly identical to spectrum E in Fig. 4 for GaN on sapphire.

Hall-effect measurements using the Van der Pauw geometry revealed that the unintentionally doped GaN films on SiC were highly n-type (n_D-n_A >10^{19} cm^{-3}). The highest observed room temperature Hall mobility for these films was 42 $cm^2/V{\cdot}s$. The average Van der Pauw resistivity was $1{\times}10^{-2}$ $\Omega{\cdot}cm$. Residual nitrogen vacancies are likely to be the cause of the high net n-type behavior.

D. Conclusions

High quality GaN thin films have been deposited directly on vicinal, Si-face (6H)-SiC(0001) substrates without the aid of a low-temperature buffer layer. The near-band-edge PL peaks revealed an apparent shift to lower energies with decreasing GaN film thicknesses. These shifts were not observed for films deposited on sapphire. Also, the surface morphologies and PL spectra of GaN films on sapphire and C-face SiC(0001) wafers were similar to each other but unlike those of films deposited on the Si-face substrates.

E. Future Research Plans and Goals

In order to increase the deposition rates of the III-V nitrides, a pancake-style susceptor will be used in place of the current barrel design. Low-temperature AlN and GaN buffer layers will be utilized to investigate their effects on the microstructural and electrical qualities of the films. Both polar planes of SiC(0001) will be examined. Efforts will be made to identify and reduce the causes of the high net carrier concentrations in the unintentionally doped GaN films. Concurrently, a p- and n-type dopant study will be initiated for both GaN and AlN.

F. References

1. R. F. Davis, Physica B **185**, 1 (1993).
2. S. Yoshida, S. Misawa and S. Gonda, Appl. Phys. Lett. **42**, 427 (1983).
3. S. Yoshida, S. Misawa and S. Gonda, J. Vac. Sci. Technol. **B1**, 250 (1983).
4. H. I. Amano, N. Sawaki, I. Akasaki and Y. Toyoda, Appl. Phys. Lett. **48**, 353 (1986).
5. I. Akasaki, H. I. Amano, Y. Koide, K. Hiramatsu and N. Sawaki, J. Cryst. Growth **98**, 209 (1989).
6. T. Lei, M. Fanciulli, R. J. Molnar and T. D. Moustakas, Appl. Phys. Lett. **59**, 944 (1991).
7. S. Nakamura, M. Senoh and T. Mukai, Jpn. J. Appl. Phys. **30**, L1708 (1991).
8. H. Amano, M. Kito, K. Hiramatsu and I. Akasaki, Jpn. J. Appl. Phys. **28**, L2112 (1989).
9. S. Nakamura, T. Mukai, M. Senoh and N. Iwasa, Jpn. J. Appl. Phys. **31**, L139 (1992).
10. C. Wang and R. F. Davis, Appl. Phys. Lett. **63**, 990 (1993).
11. F. R. Chien, private communication (1994).

12. N. Kuwano, *et. al.*, J. Cryst. Growth **15**, 381 (1991).
13. M. E. Lin, B. N. Sverdlov and H. Morkoc, Appl. Phys. Lett. **63**, 3625 (1993).
14. I. Akasaki and H. I. Amano, "Photo- & cathodoluminescence of GaN and $Al_XGa_{1-X}N$," in *Properties of Group III-Nitrides*, J. Edgar, ed., to be published.
15. T. Sasaki, T. Matsuoka and A. Katsui, Appl. Surf. Sci. **41/42**, 504 (1989).

III. Luminescence Studies of the GaN, AlN and Their Solid Solutions

A. Introduction

Luminescence is the emission of photons due to excited electrons in the conduction band decaying to their original energy levels in the valance band. The wavelength of the emitted light is directly related to the energy of the transition, by E=hv. Thus, the energy levels of a semiconductor, including radiative transitions between the conduction band, valance band, and exciton, donor, and acceptor levels, can be measured.[1,2]

In luminescence spectroscopy, various methods exist to excite the electrons, including photoluminescence (photon excitation) and cathodoluminescence (electron-beam excitation). In each technique, signal intensity is measured at specific wavelength intervals using a monochrometer and a detector. The intensity versus wavelength (or energy) plot can then be used to identify the characteristic energy band gap and exciton levels (intrinsic luminescence) of the semiconductor, and the defect energy levels (extrinsic luminescence) within the gap.[1]

Both photo- and cathodoluminescence analysis has been performed on AlN, GaN, and $Al_xGa_{1-x}N$ semiconductors.[3-15] Much of the work has been in measuring the low temperature GaN luminescence peaks. Work on AlN has been limited by the energy gap of 6.2 eV, which corresponds to a wavelength (200 nm) that is lower than most of the optical light sources. An excimer laser using the ArF line (193 nm) could possibly be used, although no one has attempted this to date. However, cathodoluminescence can be used on AlN.

Few time-resolved luminescence measurements have been performed on AlN and GaN. In a time-resolved measurement a pulsed source is used to excite the sample, and the luminescence is measured at short sampling intervals after the pulse. The result is an intensity vs. time plot. Time resolved spectroscopy is useful for separating the emission bands of the investigated samples with different decay times. It is often used to measure donor-acceptor recombination rates and minority carrier lifetimes.

Depth-resolved information can be obtained using cathodoluminescence, since generation depth varies with beam voltage. This technique is particularly useful for studying ion implanted semiconductors and layered structures.

B. Experimental Procedures

A combined photo- and cathodoluminescence system is used to measure the luminescence from the III-V Nitrides. A schematic view is shown in Fig. 1, and a block diagram is shown in Fig. 2. Each sample is attached to a cryostat that allows for a test temperature range of 4.2 to 400 K. A McPherson model 219 vacuum monochrometer

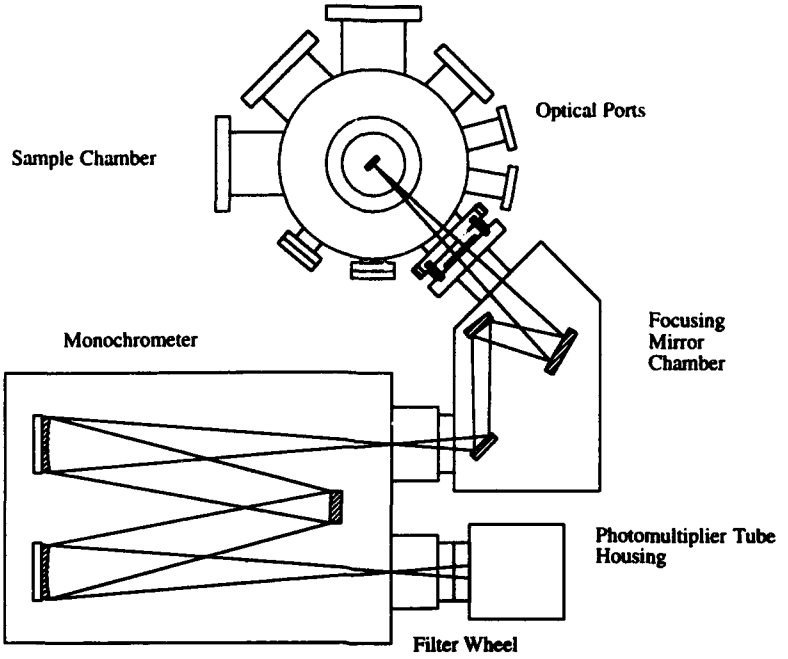

Figure 1. Schematic view of combined photo- and cathodoluminescence system.

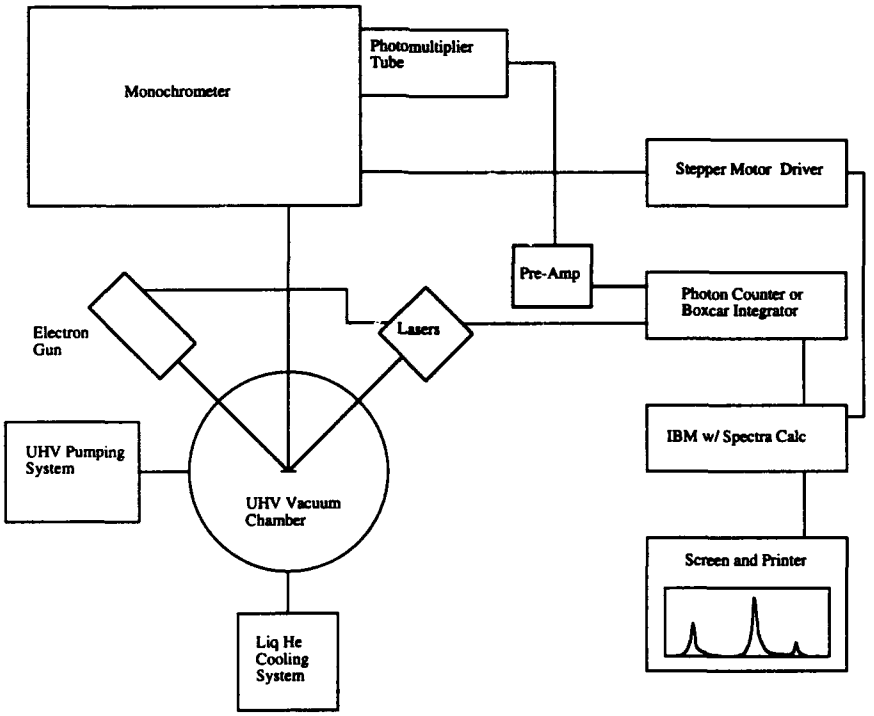

Figure 2. Block diagram of combined photo- and cathodoluminescence system.

with a focusing mirror chamber is used to collect the emitted light. The focal length of the monochrometer is .5 m, with a wavelength resolution of .04 nm at 313.1 nm. A photon counting detection scheme is used to measure the light intensity, using a photomultiplier tube that is most efficient from 185-600 nm. A lock-in amplifier will soon be added for wavelength laser that operates at a wavelength of 325 nm (3.8 eV), with a power of 15 mW. It is used for PL tests of GaN, but a lower wavelength source is needed to test the full range of the $Al_xGa_{1-x}N$ solid solutions. A pulsed excimer laser is proposed as the other optical source; it operates at wavelengths of 193 nm (6.4 eV) and 248 nm (5.0 eV).

A Kimball Physics electron gun is used for cathodoluminescence measurements. It has maximum beam voltage of 10 keV and a maximum beam current of 450 uA. By varying the beam voltage it is possible to perform depth-resolved spectroscopy.

The beam blanking capability of the electron gun will allow for time-delay studies of the semiconductors.

C. Results and Discussion

Photoluminescence measurements were performed on GaN films grown via CVD on both 6H-SiC and sapphire substrates. Each test was performed at 20 K. The results for films of various thicknesses is shown in Fig. 3. For the thickest (1.2 μm) GaN films (Fig. 3 (D) and (F)) the highest energy peaks are at 357.6 nm (3.471 eV). These peaks are attributed to the recombination of donor bound excitons.[3] Figure 3 also shows a shift in this peak to a lower energy (higher wavelength) as film thickness decreases. For the thinnest film tested (210 nm) the peak is at 368 nm (3.37 eV). For GaN on sapphire at a similar thickness the peak shift is not as strong, with the peak at 359 nm (3.457 eV). This result is expected, since the large lattice mismatch of GaN on sapphire results in film relaxation at a lower thickness.

There is also a second, lower energy peak in all of the samples, it is located at 375-378 nm (3.31-3.28 eV) for all the samples. This feature does shift much with film thickness for the GaN films on either substrate. It is tentatively designated as a donor-acceptor (DA) transition. It is also possible that this transition is due to yet unidentified defects within the film, and tests on thicker samples will be needed for positive identification of this feature.

In each of the samples tested there is a broad emission band centered at 2.2-2.3 eV, similar to that seen in Fig. 4. This is a common feature of GaN films, and its origin is still up for debate.[16] Recent work suggests a donor-acceptor pair (DAP) recombination of electrons from N vacancies (deep donor states) and holes from C-related acceptors states.[17]

The photoluminescence of GaN grown on the $(0001)_C$ and $(0001)_{Si}$ planes of 6H-GaN was also investigated. Each film was 210 nm thick, and the tests were performed at 15 K. The results are shown on Fig. 4. The near-band gap peak for the GaN on the C-plane is at 360 nm,

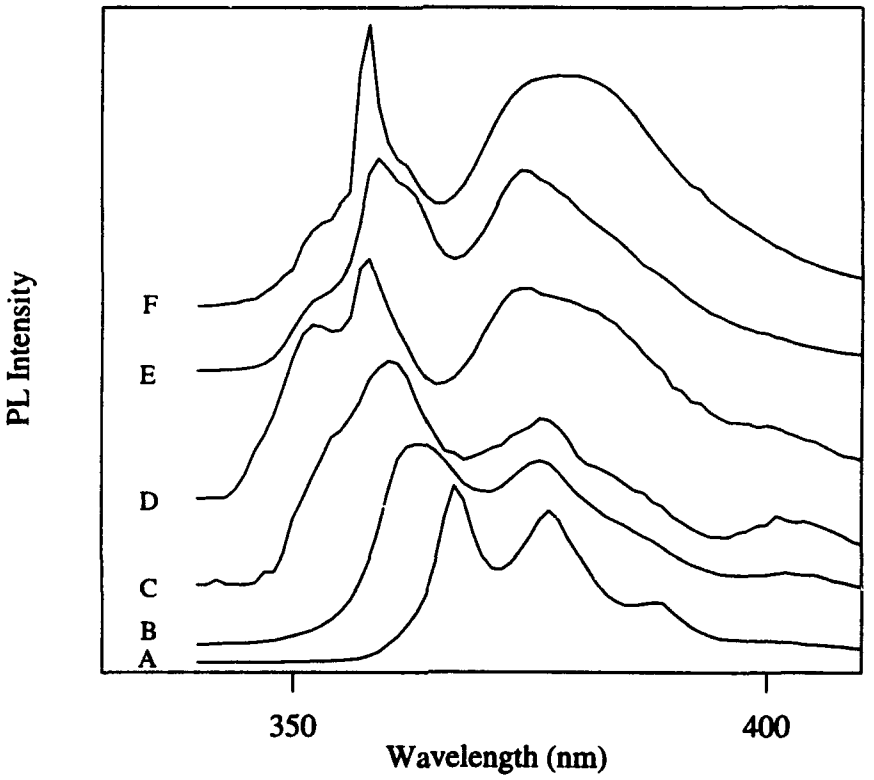

Figure 3. PL spectra comparing (A) .21 μm (B) .36 μm (C) .5 μm and (D) 1.2 μm GaN films on SiC with (E) .24 μm and 1.2 μm GaN films on sapphire.

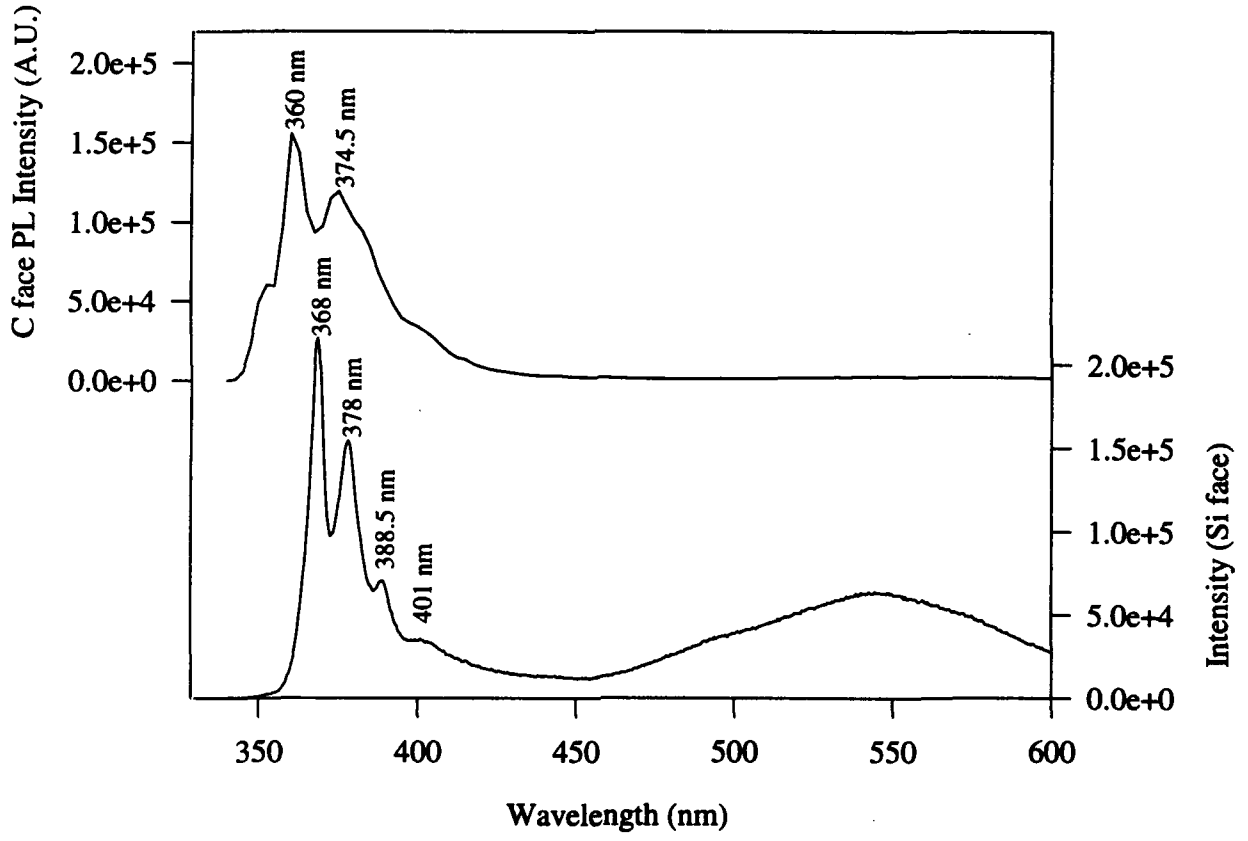

Figure 4. Comparison of the PL spectra for GaN on the Si and C planes of SiC.

and for the Si-plane it was at 368 nm. These results are similar to the GaN films on sapphire and SiC [Figs 3(E) and (A)]. Figure 4 also shows that the broad emission peak at 2.2-2.3 eV is most intense for the film grown on the Si-plane of SiC, and this is also the case when comparing GaN grown on SiC and sapphire (not shown). These results are not unexpected, as similar results for thicker GaN films were seen by other investigators.[18]

The GaN film on the Si-plane of SiC [Fig. 4] also exhibited sharp peaks at 378 nm (3.28) and 388.5 nm (3.2 eV), with a shoulder at 401 nm (3.09 eV). The last two peaks are believed to be phonon replicas of the previously discussed (DA) transition seen at 3.28 eV. These features are not seen in the thicker GaN films because of the broadness of the peak at 3.28-3.31 eV.

D. Conclusions

Photoluminescence tests have been performed on GaN films grown via CVD on both 6H-SiC and sapphire substrates. All of these films were thin, ranging from .21 to 1.2 μm. Tests were performed at 15-20 K. For the thickest samples (1.2 μm) a main peak attributed to recombination of donor bound excitons was seen at 357.6 nm. This peak shifted to higher wavelength as film thickness decreased. A second peak seen at 375-378 nm was seen all the samples, this was tentatively assigned to Donor-Acceptor transitions. A third broad emission band centered at 2.2-2.3 eV was seen in all the samples tests.

E. Future Research Plans and Goals

Thick GaN films (>2μm) with buffer layers will be studied at low temperature to test the true film quality. Using these results it will be easier to understand and verify the current data for the films tested to date. The change in luminescence as a function of film thickness will further be investigated, for both SiC and sapphire substrates with and without buffer layers. The effect of temperature on luminescence will also be studied for the range of 10 K to 450 K, and the results will be used to study the activation energy for the donor-bound excitons.

Cathodoluminescence will be used to study $Al_xGa_{1-x}N$ alloys grown by both CVD and GS-MBE. A excimer waveguide laser will also be added to the system, with a peak emission at 193 nm. This will allow for photoluminescence measurements of AlN, which has not been done yet above the band gap. Cathodoluminescence will also be used to perform depth-resolved spectroscopy of GaN, AlN and their alloys.

F. References

1. B. G. Yacobi and D. B. Holt, *Cathodoluminescence Microscopy of Inorganic Solids*, Plenum Press, New York (1990).

2. M. D. Lumb, Ed., *Luminescence Spectroscopy*, Academic Press, New York (1978).
3. S. Strite and H. Morkoç, J. Vac. Sci. Technol. B **10** (4), 1237-1266 (1992).
4. R. A. Youngman and J. H. Harris, J. Am. Ceram. Soc. **73** (11), 3238-46 (1990).
5. M. A. Kahn, R. A. Skogman, J. M. Van Hove, S. Krishnakutty, and R. M. Kolbas, Appl. Phys. Lett. **56** (9130), 1257-59 (1990).
6. V. F. Veselov, A. V. Dobrynin, G. A. Naida, P. A. Pundur, E. A. Slotensietse, and E. B. Sokolov, Inorganic Materials **25** (9), 1250-4 (1989).
7. J. N. Kuznia, M. A. Kahn, D. T. Olson, R. Haplan, and J. Freitas, J. Appl. Phys. **73** (9), 4700-4702 (1993).
8. M. R. H. Khan, N. Sawaki and I Akasaki, Semiconductor Science and Technol[illegible] 7, 472-7 (1992).
9. K. Maier, J. Schneider, I. Akasaki, and H. Amano, Jpn. J. Appl. Phys. **32** (6), 8[illegible] (1993).
10. I. Akasaki, and H. Amano, J. Crystal Growth **99**, 375-80 (1990).
11. S. Yoshida, H. Okumura, S. Misawa, and E. Sakuma, Surf. Sci. **267** (7), 50-53 (1992).
12. S. Nakamura, T. Mukai, and M. Senoh, Jpn. J. Appl. Phys., **31** (9) 2883-90 (1992).
13. S. Nakamura, N. Iwasa, T. Mukai, and M. Senoh, Jpn. J. Appl. Phys. **31** (5), 107-15 (1992).
14. S. Nakamura, T. Mukai, and M. Senoh, Jpn. J. Appl. Phys. **30** (12A), 1998-2001 (1991).
15. S. Strite, J. Ruan, Z. Li, N Manning, A. Salvador, H. Chen, D. J. Smith, W. J. Choyke, and H. Morkoç, J. Va. Sci. Technol. B **9** (4), 1924-29 (1991).
16. E. R. Glaser, T. A. Kennedy, H. C. Crookham, J. A. Freitas, Jr., M. Asif Khan, D.T. Olson, and J. N. Kuznia, Appl. Phys. Lett. **63** (19), 2673-2675 (1993).
17. E. R. Glaser, T. A. Kennedy, J. A. Freitas, Jr., M. Asif Khan, D. T. Olson, and J. N. Kuznia, from the Fifth International Conference on Silicon Carbide and Related Materials in Washington, D.C., Nov. 1993, to be published in the "International Institute of Physics Conferences" Series.
18. T. Sasaki, T. Matsuoka, A. Katsui, Appl. Surf. Sci. **41/42**, 504-508 (1989).

IV. Nitride Devices and Use of NH_2 for Film Growth

A. Introduction

AlN, GaN, and AlGaN thin films are presently grown by various techniques including MOCVD, MOVPE, and GSMBE. Although the quality of AlN films have been nearly optimized, the quality of GaN films currently need to be improved, particularly GaN films grown by modified (ECR) GSMBE. Presently, the microstructures of GSMBE grown GaN exhibit columnar features and relatively poor surface morphologies. The columnar features are likely caused by the lattice mismatch between the AlN buffer and GaN film, and the subsequent stress build up that occurs as the film is grown thicker. The poor surface morphology may be caused by the detrimental interaction of high energy ionized N species with the newly deposited GaN surface during growth. The highly energetic ionized N results from the use of ECRs in GSMBE growth processes [1,2]. These energetic ions are thought to cause point defects in the film surface adding to the poor microstructures exhibited in GaN films.

InN and InGaN have also been successfully grown, however the microstructural quality has also been poor. InN poses an additional major obstacle to quality film growth, namely its poor thermal stability. By use of the lower substrate growth temperatures offered by GSMBE, this obstacle is easily overcome relative to growth techniques such as MOVPE and MOCVD where film deposition is performed at higher temperatures. The problem encountered using GSMBE is again the susceptibility of the film surface to damage caused by the high energy ionized N species.

Therefore, in order to obtain quality GaN and InN films grown by MBE, an alternative method of producing atomic nitrogen which minimizes or eliminates the undesirable production of high energy ionic nitrogen needs to be developed. This report presents the design and development of a high temperature ammonia cracking source for production of atomic nitrogen as an alternative to the ECR source in GSMBE.

B. Experimental Procedure

The ammonia cracking source being manufactured by Effusion Science Inc. will fit completely in the sleeve of our currently unused MBE effusion cell (2.25" diameter) [3]. The ammonia will enter the cracker cell and will decompose by means of a single bounce delivery off of a wide-area catalytic rhenium filament. Al, Ga, and In fluxes will be provided by the normal MBE effusion cells. Due to the pumping requirements for ammonia and its byproducts, a turbomolecular pump will be installed to provide the required high vacuum environment. A throttle valve will be used on the inlet to the pump allowing for control of the deposition chamber pressure. AlN, GaN, InN, and their solid solutions will be grown at

various temperatures and pressures on SiC and sapphire to optimize the growth rate and film microstructure.

C. Discussion

The use of cracking ammonia as a source of nitrogen is not new to the field of III-V nitride growth. It is the current method used in growth techniques such as MOCVD and MOVPE where ammonia is cracked on the surface of the substrate, requiring relatively higher growth temperatures to achieve efficient nitrogen production. Reactive molecular beam epitaxy has also used the cracking of ammonia on the substrate as a nitrogen source. Another technique recently used was hot filament enhanced CVD [4,5]. In this process, it is surmised that the catalyzed film growth is initiated through the decomposition of ammonia and subsequent production of NH radicals by a heated tungsten filament. These products trigger further reactions which react with the metalorganic gas to form precursors to film deposition. These precursors then decompose on the heated substrate resulting in film growth [5]. The decomposition of ammonia on various filament surfaces at high temperatures has shown that the two primary reactions that occur are:

$$1)\quad NH_3 + M \rightarrow NH_2 + H + M$$
$$2)\quad NH_3 + H \rightarrow NH_2 + H_2$$

In the case of the catalyzed CVD growth, reaction 2 is enhanced by the addition of hydrogen to the reaction chamber between the tungsten filament and the heated substrate to aid in the production of NH_2. It is the secondary reactions, primarily the formation of NH radicals, that next occur which are responsible for precursor formation with the metalorganic mentioned above [4-6]. Examples of these secondary reactions include:

$$3)\quad NH_2 + H \rightarrow NH + H_2$$
$$4)\quad NH_2 + NH_2 \rightarrow NH + NH_3$$

Ammonia Gas Cracker. The choice of rhenium as the catalytic filament was made for two reasons. First, rhenium catalysts are exceptionally resistant to passivation from gases such as nitrogen, thereby limiting additional power requirements to maintain constant energy transfer to the ammonia over the lifetime of the filament [7]. Second, hydrogen atoms have been detected in ammonia decomposition reactions on rhenium filaments heated to high temperatures approaching 2000 K [8]. Therefore, it should not be necessary to add hydrogen from some other source to aid in the production of NH_2. The secondary reactions producing the NH radicals are also expected to react with the group III species at the growth surface in MBE, resulting in film growth.

Investigations of the pyrolysis of ammonia suggest that atomic nitrogen produced by the cracking of ammonia occurs as a result of the secondary and tertiary reactions, and the total expected mole fraction for atomic nitrogen is on the order of 10^{-5} [8]. To reduce the chance of any resulting atomic nitrogen recombining into molecular nitrogen, the flow of ammonia through the cracker cell will be designed with a single bounce delivery path, thereby limiting the number of collisions each N atom undergoes after cracking on the filament prior to reaching the substrate surface.

D. Future Research Plans and Goals

Over the next few months we will be installing the ammonia cracker cell and supporting equipment. Preliminary work will concentrate on optimizing the growth of films by this source of nitrogen. These films will be compared to films grown presently by modified (ECR) GSMBE. Once we have established that this source of nitrogen is practical for film growth, we will employ the technique for development of optical devices including blue LEDs.

E. References

1. Z. Sitar, M. J. Paisley, D. K. Smith and R. F. Davis, Rev. Sci. Instrum. **61**, 2407 (1990).
2. T. D. Moustakas, T. Lei and R. J. Molnar, Physica **B185**, 36 (1993).
3. C. Bichrt, W. D. Braddock, Effusion Science Inc., private communication.
4. J. L. Dupuie and E. Gulari, Appl. Phys. Lett. **59**, 549 (1991).
5. J. L. Dupuie and E. Gulari, J. Vac. Sci. Technol. **A10** (1), 18 (1991).
6. G. S. Selwyn and M. C. Lin, Chemical Physics **67**, 213 (1982).
7. Handbook of Chemistry and Physics **73**, 4-24 (1992).
8. S. N. Foner and R. L. Hudson, J. Chem. Phys. **80** (9), 4013 (1984).

V. Application of Epitaxial Aluminum Nitride (AlN) in Metal-Insulator-Semiconductor Structures

A. Introduction

The large band-gap (6.2eV) and good thermal stability (0.05 Torr equilibrium vapor pressure of nitrogen at 1500°C) indicate that AlN films have considerable potential as a dielectric in electronic devices. There are several published papers [1–4] which describe the investigations and the applications of AlN films as insulators in several MIS structures containing Si and GaAs. However, in all these studies the AlN films were polycrystalline.

We have shown in previous reports that AlN films with low defect densities can be epitaxially deposited on SiC substrates by the use of a modified gas source MBE system [5]. In this paper, we have investigated the application of epitaxial AlN films as insulators in SiC MIS structures. The electrical properties of the AlN insulator layers have been studied using current voltage (I-V) and high-frequency capacitance-voltage (hf C-V) measurements.

B. Experimental Procedure

The MIS structure was fabricated using a commercial Perkin-Elmer 430 MBE system. This system consists of three parts: a load lock (base pressure of 5×10^{-8} Torr), a transfer tube (base pressure of 1×10^{-10} Torr), which also was used for degassing the substrates, and the growth chamber (base pressure of 5×10^{-11} Torr). A Knudson effusion cell with a BN crucible and a Ta wire heater was charged with 6N pure aluminum. Ultra-high purity nitrogen, further purified by a chemical purifier, was used as the sources gas. The nitrogen was excited by an ECR plasma source, which was designed to fit inside the 2.25 inch diameter tube of the source flange cryoshroud.

The substrates were n-type ($n=6.4\times10^{16}$ cm^{-3}), vicinal α(6H)-SiC(0001) wafers oriented 3-4° towards [1120] and supplied by Cree Research Inc. An ohmic Ni contact was deposited on the backside. Prior to deposition, the substrates were cleaned by a standard degreasing procedure, chemically cleaned in a 10% HF solution for five minutes, mounted on a 3-inch molybdenum block, loaded into the system, heated to 700°C for 30 minutes in the transfer tube under UHV conditions to remove surface hydrocarbons and transferred into the deposition chamber.

A 125 Å thick of epitaxial AlN was deposited on the α-SiC wafer at 1100°C, followed by *in situ* deposition of Al-metal layer at room temperature. The details of the epitaxial deposition conditions of AlN film can be found in Ref. [5]. To form MIS diodes, the top Al-layer was patterned by standard lithographic etching techniques as circular dots of radius 50 μm and annealed at 400°C for half hour in the vacuum. The schematic diagram of the MIS structure was shown in Fig. 1.

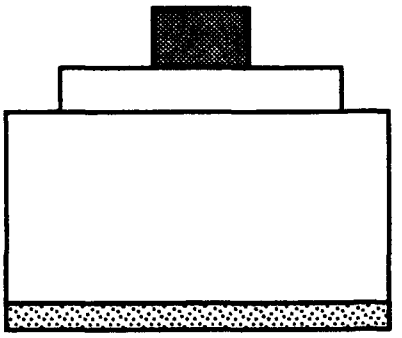

Figure 1. Schematic diagram of AlN MIS diode.

Direct I-V and hf C-V characteristics of the MIS structures at different temperature were characterized using a Hewlett Packard 4145 Semiconductor Parameter Analyzer and a Keithley M590CV Analyzer, respectively.

C. Experimental Results

The experimental I-V curves of the MIS structure at two different temperatures are shown in Fig. 2. Rectifying behavior was observed. The forward bias current increased with an increase of the forward bias voltage. The breakdown field of the AlN MIS structure was ≈ 13.4 MV/cm at room temperature; the value was slightly smaller, 13 MV/cm, at 300°C. The revise bias currents are very small for both temperatures and no breakdown occurred even for the field larger than 70 MV/cm.

The results of hf C-V measurements of the MIS diode are shown in Fig. 3. These measurements were made using a 100 kHz AC signal. Figure 3 indicates that the diode could be swept from accumulation to inversion. Hysteresis in the C-V trace was observed when the voltage ramp direction was reversed. The diode also exhibited a positive flat band voltage. From the film thickness and accumulation capacitance data, the dielectric constant of AlN insulator layer at 100kHz was estimated as ~14, which is higher than what has been reported [3,6].

D. Discussion

The recent advances of III-V nitride film quality have resulted in the successful fabrication of a variety of III-V nitride based devices [7-9]. It is expected that it will become important to study and develop the proper insulating material for III-V nitride devices. For many years, the potential of using AlN as dielectric insulator due to its large band gap and good thermal stability has been realized. There were several reported investigations of the use of AlN as an insulator in MIS structures. However most of the work conducted to date has

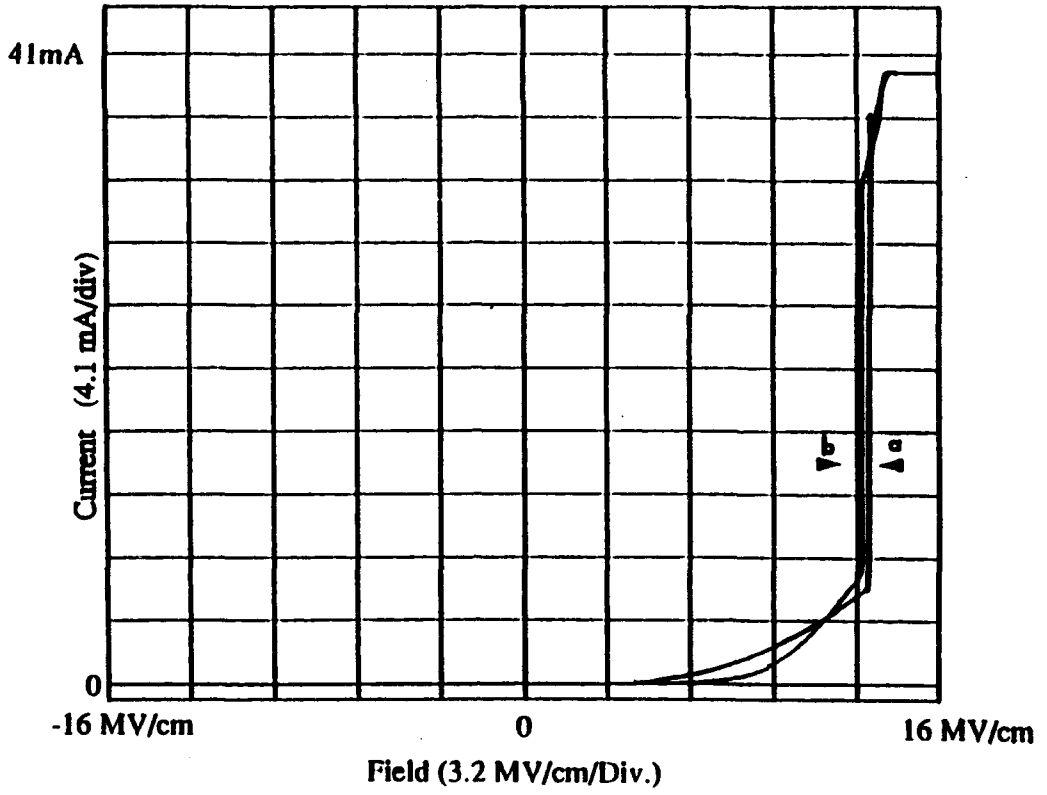

Figure 2. I-V curve for AlN MIS diode measured at (a) room temperature; (b) 300°C.

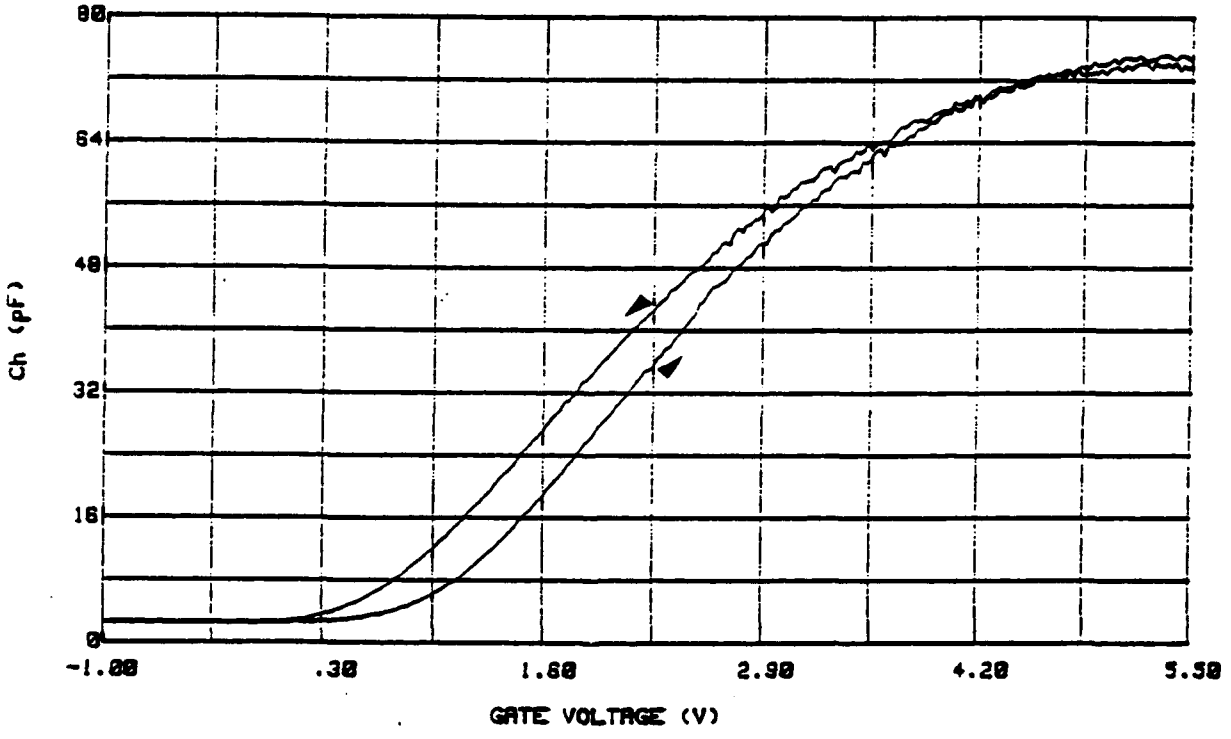

Figure 3. C-V curve of AlN MIS diode measured at 100 kHz of frequency.

been on Si or GaAs substrates, and the AlN film films were polycrystalline. We are for the first time reporting the use of monocrystalline epitaxial AlN films as the insulator in a SiC MIS structure. The dielectric properties of AlN have been studied and the AlN MIS structure has been demonstrated to be operative at high temperature (300°C). The significance of this work is that the application of epitaxial AlN as an insulator can simplify the III-V device process. However, this study is preliminary. More detailed investigations are needed to fully understand the dielectric properties of the AlN films, including the determination of the interface state densities and reducing the methods for the leakage currents before they can be successfully used in device structures.

As we have shown above, the AlN MIS structure exhibited both rectification behavior and unwanted leakage currents. These phenomena may be explained using the band diagram in Fig. 4. Under reverse bias, the SiC semiconductor substrate is in the depletion mode, therefore, the majority of the applied voltage is dropped across the depletion region, as shown in Fig. 4(b). Under forward bias, the semiconductor region is in an accumulation state; therefore, a large part of the voltage is across the barrier, which causes severe band bending at the interface, as shown in Fig. 4(c). This band bending reduces the effective barrier height and increases the probability of tunneling through the thin barrier region. Both of these factors lead to a large leakage currents. It is expected that by increasing the AlN thickness, and using the metals with higher work function, the probability of band bending and tunneling would be suppressed and the leakage current reduced.

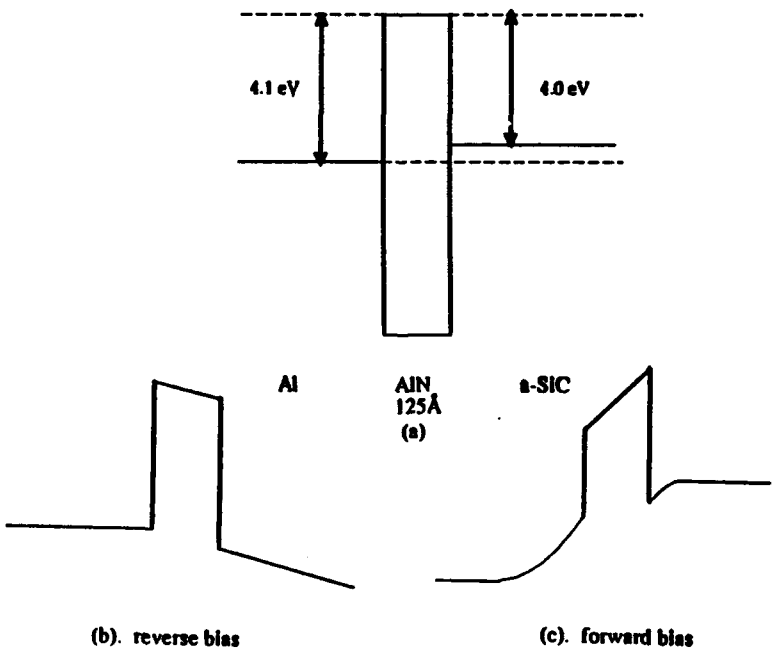

Figure 4. Band diagram of AlN MIS structure under the bias conditions: (a) no bias; (b) reverse bias; (c) forward bias.

E. Summary

A preliminary investigation of the use of monocrystalline epitaxial AlN in an SiC MIS structure has been conducted. The breakdown field of AlN was estimated to be 13.4 MV/cm at room temperature. At 300°C, the breakdown decreased slightly to 13 MV/cm. Capacitance-voltage characteristics showed that the diode could be swept from accumulation to inversion. The dielectric constant has been estimated as ~14.

F. References

1. S. Mirsch and H. Reimer, Phys. Stat. Sol. 11, 631 (1972).
2. E. A. Irene and V. J. Silvestri, J. of Electronic Materials Vol.4, 409 (1975).
3. T. L. Chu and R. W. Kelm, J. Electrochem. Soc. 122, 995 (1975).
4. Y. Mochizuki, M. Mizuta, S. Fujieda and Y. Matsumoto, J. Appl. Phys. 67, 2466 (1990).
5. C. Wang, K. S Ailey, K. L. More and R.F. Davis, in press (1993).
6. A. T. Collins, E. C. Lightowlers and P. J. Dean, Phys. Rev. 158, 833 (1967).
7. R. F. Davis, Proc. IEEE 79, 702 (1991).
8. A. M. Khan, J. K. Kuzina and R. T. Olson, Appl. Phys. Lett. 62, 1786 (1993).
9. S. Strite and H. Morkoc, J. Vac. Sci. Technol. B10, 1237 (1992).

VI. *Distribution List*

Mr. Max Yoder Office of Naval Research Electronics Division, Code: 314 Ballston Tower One 800 N. Quincy Street Arlington, VA 22217-5660	3
Administrative Contracting Officer Office Of Naval Research Resident Representative The Ohio State University Research Center 1960 Kenny Road Columbus, OH 43210-1063	1
Director, Naval Research Laboratory ATTN: Code 2627 Washington, DC 20375	1
Defense Technical Information Center Bldg. 5, Cameron Station Alexandria, VA 22314	2
Washington Headquarters Services ATTN: Dept. Acctg. Division Room 3B269, The Pentagon Washington, DC 20301-1135	2